Academic Journal of Science and Technology
ISSN: 2771-3032 | Vol. 21, No. 1, 2026

Research on Internal Flow Field Simulation and Structural Optimization of Mesh Belt Dryer

Jiahui Wang[1], Lin Dong[2,*], Huan Zhang[3], Cheng Yin[1], Peng Yu[1], Zhenghai He[1]

[1] School of Mechanical Engineering, Xihua University, Chengdu, Sichuan 610039, China
[2] School of Aerospace and Intelligent Equipment, Xihua University, Chengdu, Sichuan 610039, China
[3] China Shipbuilding Group Yangtze River Technology Co., Ltd, Chongqing 404002, China

[*] Corresponding author: lin.dong@mail.xhu.edu.cn)

Abstract: In order to solve the problem that the internal airflow and temperature field distribution of the belt dryer are uneven, resulting in poor drying quality, this paper conducts 3D modeling and flow field simulation analysis of the drying chamber of the three-layer belt dryer based on computational fluid dynamics (CFD). The velocity and temperature fields of the original drying chamber were numerically simulated by using the Realizable k-ε turbulence model and the porous medium model. The results show that in the original structure, the average velocities on the three-layer mesh belts are 0.93 m/s, 1.09 m/s, and 0.88 m/s, with non-uniformity coefficients of 78.36%, 56.95%, and 47.53%, respectively; the average temperatures are 60.18°C, 58.34°C, and 57.51°C, with non-uniformity coefficients of 14.84%, 24.79%, and 15.03%. By adding an air distributor below the air inlet and comparing different perforation sizes, it was found that the optimal optimization effect is achieved when the perforation diameter is **40 mm**: the average velocities on the three-layer mesh belts increase by 0.55 m/s, 0.27 m/s, and 0.27 m/s, while the non-uniformity coefficients decrease by 35.85%, 21.09%, and 27.06%; the average temperatures rise by 4.34°C, 5.49°C, and 5.64°C, and the non-uniformity coefficients drop by 9.87%, 14.92%, and 6.67%. This research provides a theoretical basis for the structural optimization of mesh belt dryers.

Keywords: Mesh belt dryer; Computational fluid dynamics; flow field simulation; Wind equalizer.

1. Introduction

In actual production, the drying of bitter gourd is often conducted in large batches, typically using a mesh belt dryer. Operating continuously, the mesh belt dryer is highly suitable for vegetables and Chinese medicinal materials that have high moisture content and require post-drying structural integrity. However, during the actual production process, the moisture unevenness of the dried products is often high. This is because the airflow distribution within the drying chamber during the drying process is uneven, leading to suboptimal drying results.

Computational Fluid Dynamics (CFD) technology is utilized to simulate the flow field inside the drying chamber of the mesh belt dryer. CFD is a technique that uses computers for numerical simulation and graphical display, allowing for the visualization of temperature and velocity fields after simulation [1]. CFD is also widely applied in the design field of drying machinery, as it can simulate the internal region of the dryer to effectively ensure drying performance. The core function of Fluent software is to solve fluid dynamics governing equations through numerical methods, helping users predict fluid behavior in real scenarios, thereby optimizing designs, reducing costs, and accelerating product development [2-4].

2. Model Establishment and Simulation Methods

2.1. Geometric Model and Simplification

This study primarily targets the JNKF23001 three-layer mesh belt dryer, with dimensions of 7566 mm in length, 2068 mm in width, and 3056 mm in height. The spreading area of each layer is approximately 3 m², totaling about 9 m² for all three layers. As shown in Figure 1, the dryer mainly consists of a feeding machine, an electric heater, a three-layer mesh belt, a drying chamber, a circulation fan, a dehumidification fan, and a regenerator. The internal three-layer mesh belts move in opposite directions between adjacent layers to drop the materials from the upper layer to the lower layer sequentially. Once drying is complete, the dried product is discharged through the rear outlet, cooled, and bagged. The 3D modeling of the mesh belt dryer is shown in Figure 2.

Figure 1. Mesh belt dryer

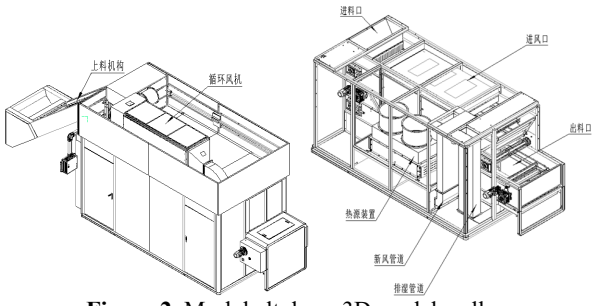

Figure 2. Mesh belt dryer 3D model wall

2.2. Mathematical Model

In fluid flow, the governing laws must comply with the laws of conservation of mass, momentum, and energy. Therefore, in fluid simulation, the "three major equations" are required to describe the basic physical laws of fluid motion: the continuity equation (mass conservation equation), the momentum conservation equation, and the energy conservation equation [5-7].

(1) Mass conservation equation

$$\frac{\partial_{\rho}}{\partial_{t}}+\frac{\partial_{(\rho u)}}{\partial_{x}}+\frac{\partial_{(\rho v)}}{\partial_{y}}+\frac{\partial_{(\rho w)}}{\partial_{z}}=0 \tag{1}$$

(2) Momentum conservation equation

$$\begin{cases}\dfrac{dv_x}{dt}=f_x-\dfrac{1}{\rho}\dfrac{\partial P}{\partial x}+\mu\left(\dfrac{\partial^2 v_x}{\partial x^2}+\dfrac{\partial^2 v_x}{\partial y^2}+\dfrac{\partial^2 v_x}{\partial z^2}\right)\\ \dfrac{dv_y}{dt}=f_y-\dfrac{1}{\rho}\dfrac{\partial P}{\partial y}+\mu\left(\dfrac{\partial^2 v_y}{\partial x^2}+\dfrac{\partial^2 v_y}{\partial y^2}+\dfrac{\partial^2 v_y}{\partial z^2}\right)\\ \dfrac{dv_z}{dt}=f_z-\dfrac{1}{\rho}\dfrac{\partial P}{\partial z}+\mu\left(\dfrac{\partial^2 v_z}{\partial x^2}+\dfrac{\partial^2 v_z}{\partial y^2}+\dfrac{\partial^2 v_z}{\partial z^2}\right)\end{cases} \tag{2}$$

(3) Energy conservation equation

$$\frac{\partial(\rho T)}{\partial x}+div(\rho \boldsymbol{u} T)=div\left(\frac{k}{C_P}gradT\right)+S_T \tag{3}$$

2.3. Porous Media Model

In the porous media model, the gas flow is mainly affected by the viscous resistance and inertial resistance from the bitter gourd. In CFD, the momentum equation for the porous media model domain [8] is shown as Equation (4).

$$S_i=\sum_{j=1}^{3}D_{ij}uv_j+\sum_{j=1}^{3}C_{ij}\left|v_j\right|v_j \tag{4}$$

When dealing with an isotropic porous media model, the resistance source term in the momentum equation can be expressed as Equation (5).

$$Re=\frac{\rho vd}{\mu} \tag{5}$$

2.4. Boundary Conditions and Solution Settings

Air Inlet Boundary Parameter Settings: Since the airflow velocity inside the drying chamber is relatively low, the air is treated as an incompressible fluid. A velocity inlet condition is applied at the air inlet. Based on the optimal hot air drying process for bitter gourd obtained previously, the temperature is set to 65°C and the wind speed is set to 1.5 m/s.

Air Outlet Boundary Parameter Settings: A pressure outlet setting is adopted at the air outlet. Because the airflow in the drying chamber develops fully and is discharged through the outlet, the pressure at the outlet is equivalent to the external atmospheric pressure, i.e., 103,125 Pa [9].

Porous Media Region Parameter Settings: In this simulation, the bitter gourd spread on the mesh belt is simplified into a porous media model. It requires the configuration of porosity, viscous resistance coefficient, and inertial resistance coefficient. The results are a porosity of 72.8%, a viscous resistance coefficient of 1,630,558.36, and an inertial resistance coefficient of 477.64.

Wall Boundary Parameter Settings: Because there is an insulation layer outside the drying chamber, the drying region walls are set as no-slip adiabatic walls.

3. Flow Field Analysis of the Original Structure

Calculations were performed for the three-layer mesh belt. Using the equidistant point sampling method in the CFD-Post post-processing tool within Fluent, 100 sample points were taken for each layer, as shown in Figure 3.

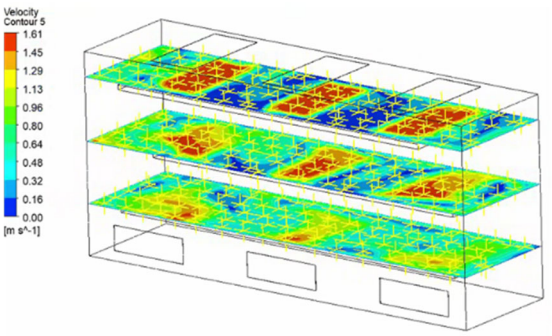

Figure 3. Three layer mesh point cloud map

By analyzing the airflow streamline diagram of the drying chamber and the airflow contour maps of the three-layer mesh belts, it is observed that the wind speed is higher near the air inlet, while other regions experience eddy currents leading to lower wind speeds. This phenomenon is most severe on the first layer of the mesh belt.

Analyzing the average velocity and non-uniformity coefficient from the wind speed contour maps reveals that from the first layer to the third layer, the average velocities and non-uniformity coefficients are: 0.93 m/s, 1.09 m/s, 0.88 m/s, and 78.36%, 56.95%, 47.53%, respectively. The average velocities and non-uniformity coefficients in the left and right views are: 0.79 m/s, 0.86 m/s, 0.97 m/s. It is clearly apparent that the airflow distribution inside the drying chamber is extremely uneven, which greatly impacts the drying effectiveness.

Analyzing the temperature contour maps on the three-layer mesh belts, the average temperatures and non-uniformity coefficients are 53.18°C, 55.34°C, 50.51°C and 14.84%, 24.79%, 15.03%, respectively. It is found that the average temperature is relatively low and has not reached the targeted temperature from the optimal drying process, although the temperature non-uniformity coefficients perform reasonably well. Therefore, it is necessary to structurally optimize the drying chamber to guarantee a proper drying effect.

4. Structural Optimization and Result Analysis

4.1. Analysis of Velocity Flow Field After Adding the Air Distributor

As seen in Figure 4, after adding the air distributor, when the hot air enters from the air inlet, it diffuses to both sides due to the obstruction of the distributor. After passing through the distributor perforations, it reaches the drying area, distributing the hot air evenly across the three-layer mesh belts. The airflow becomes significantly more uniform and its flow direction more orderly. The average velocity and non-uniformity coefficients were improved; the average velocities increased by 0.41 m/s, 0.08 m/s, and 0.09 m/s, respectively, and the non-uniformity coefficients decreased by 20.98%, 15.46%, and 19.16%, respectively.

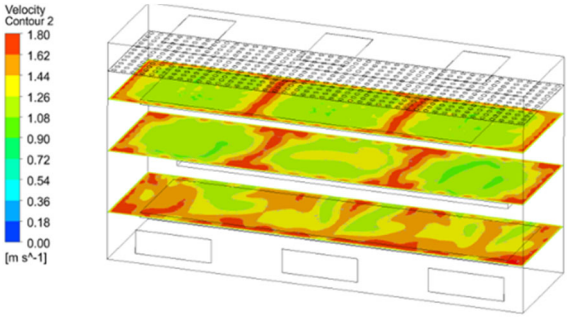

Figure 4. Three layer velocity cloud map after adding a uniform wind plate

4.2. Effect of Adding the Air Distributor on the Temperature Field

As seen in Figure 5, compared to the temperature field without the air distributor, the overall temperature uniformity of the drying chamber improves significantly after its addition. The average temperatures increased by 3.73°C, 4.88°C, and 6.10°C, and the non-uniformity coefficients dropped by 9.49%, 14.15%, and 6.62%. This yields a much more uniform temperature field inside the drying chamber. The average temperatures on the three-layer mesh belts are maintained within the reasonable range of 65°C (the optimal bitter gourd drying process), and the non-uniformity coefficients remain at or below roughly 10.64%. This demonstrates that the temperature difference across various points is small, presenting a clear enhancement in drying performance.

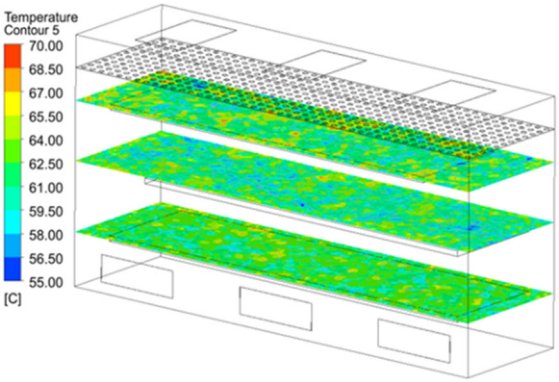

Figure 5. Temperature cloud map after adding a uniform air plate

4.3. Effect of Changing Perforation Size on the Temperature Field

Since adding the air distributor greatly increases the temperatures on the mesh belts compared to the unoptimized drying chamber, this section compares the temperature fields when the perforations are set to 40 mm and 30 mm to select the optimal structure. The results are shown in Table 1:

Table 1. Temperature comparison between 30 mm and 40 mm uniform air holes

Contour Map Position	1	2	3	1	2	3
	40 mm Perforation			30 mm Perforation		
Average Temperature (°C)	64.52	63.83	63.15	63.92	63.66	62.71
Non-uniformity Coefficient (%)	4.97	9.87	8.36	4.86	9.63	7.94

When a perforation diameter of 40 mm is selected, both the airflow intensity and the temperature field are guaranteed to meet the required standards. Therefore, adding an air distributor with 40 mm perforations below the air inlet is the chosen path for structural optimization.

5. Conclusion

Through contour map analysis in CFD-post, it was found that the average velocities and non-uniformity coefficients on the three-layer mesh belts of the original structure are 0.93 m/s, 1.09 m/s, 0.88 m/s, and 78.36%, 56.95%, 47.53%, respectively. The average velocities and non-uniformity coefficients in the left and right views are: 0.79 m/s, 0.87 m/s, and 0.97 m/s. The average temperatures and temperature non-uniformity coefficients of the three-layer mesh belts are 60.18°C, 58.34°C, 57.51°C, and 14.84%, 24.79%, 15.03%. The data indicate that the drying effect in the drying area of the mesh belt dryer is not ideal, necessitating structural optimization.Ultimately, it was determined that when the uniform perforation is 40 mm, the average velocities on the three-layer mesh belts improve by 0.55 m/s, 0.27 m/s, and 0.27 m/s, while the non-uniformity coefficients decrease by 35.85%, 21.09%, and 27.06%. The temperature uniformity also improves, with average temperatures rising by 4.34°C, 5.49°C, and 5.64°C, and non-uniformity coefficients dropping by 9.87%, 14.92%, and 6.67%.

Acknowledgment

This work was supported by Sichuan Science and Technology program (2026YFHZ0181).

References

[1] Li, D., & Fan, Y. (2014). *Computational fluid dynamics*. Tianjin University Press.

[2] Sun, B., Li, M., Li, M., et al. (2013). *ANSYS FLUENT 14.0 simulation analysis and optimization design* (p. 354). China Machine Press.

[3] Zhang, K., Wang, R., & Wu, L. (2010). *Fluent technology foundation and application examples*. Tsinghua University Press.

[4] Li, Q., Ji, X., Lan, Q., et al. (2022). Simulation and optimization of airflow field in white tea drying system based

on CFD. *Journal of Yunnan Normal University (Natural Sciences Edition)*, *42*(4), 6–9.

[5] Ren, Y. (2017). *Study on the characteristics of microwave-hot air combined drying of chrysanthemum and numerical simulation of its flow field distribution* (Master's/Doctoral dissertation). Henan Agricultural University.

[6] Lu, R. (2012). *Design of a vertical dryer and study on the air velocity field of its drying unit* (Master's/Doctoral dissertation). Huazhong Agricultural University.

[7] Li, Y., Ai, Y., Liu, W., et al. (2020). Simulation analysis and verification of splash lubrication for a reducer based on CFD. *Journal of Aerospace Power*, *35*(7), 1482–1488. https://doi.org/10.13224/j.cnki.jasp.2020.07.019

[8] Bao, Y. (2015). *Thermal-moisture analysis and optimization in the process of tobacco leaf baking* (Master's/Doctoral dissertation). Chongqing University.

[9] Liu, W., Li, H., Wang, S., et al. (2022). Analysis and optimization of thermal flow field uniformity in sunflower seed dryer. *Packaging and Food Machinery*, *40*(6), 83–88.